IEEE Access
Multidisciplinary | Rapid Review | Open Access Journal

Received September 15, 2019, accepted October 4, 2019, date of publication October 8, 2019, date of current version October 18, 2019.

Digital Object Identifier 10.1109/ACCESS.2019.2946167

Rateless Polar-Spinal Coding Scheme With Enhanced Information Unequal Error Protection

HAO LIANG, AIJUN LIU, (Member, IEEE), FENGYI CHENG, AND XIAOHU LIANG
College of Communications Engineering, Army Engineering University of PLA, Nanjing 210007, China

Corresponding author: Aijun Liu (liuaj.cn@163.com)

This work was supported in part by the National Natural Science Foundation of China under Grant 61671476, and in part by the Natural Science Foundation of Jiangsu Province of China under Grant BK20180578.

ABSTRACT In this paper, a rateless coding scheme with enhanced unequal error protection (UEP) property is proposed by concatenating the systematic polar code (SPC) and spinal code, where SPC is used as the outer code and spinal code is the inner code. The novel concatenated polar-spinal coding scheme is designed to provide an improved UEP for the information with different reliability requirements. At the receiver, a tail CRC-aided Bubble decoding is proposed to improve the performance of spinal codes effectively. Moreover, the rateless transmission control is designed carefully for the time-varying channels. The total complexity of joint concatenated decoding process is reduced. Simulation and analysis verify that the novel rateless polar-spinal coding scheme can provide better UEP performance for the information of each importance level in contrast to some existing UEP rateless coding schemes.

INDEX TERMS Polar codes, spinal codes, concatenation, unequal error protection, rateless coding, joint decoding.

I. INTRODUCTION

For many new radio scenarios such as 5G and Internet of Things (IoT) applications, different classes of data have various reliability requirements. The channel state information, power control signals and reconstruction parameters of image video may have higher priority level and need higher reliability. However, the conventional channel coding schemes generally assume equal importance to all the information to provide an equal error protection (EEP). Therefore the concept of unequal error protection (UEP) is proposed as an efficient solution to ensure that the most important information part will enjoy more protection. A variety of UEP schemes have been designed on basis of the existing low-density parity-check (LDPC) codes [1], turbo codes [2], rateless codes, etc.

Polar codes, invented in [3], are a family of capacity-achieving codes for binary input discrete memoryless channels (BI-DMC), which have explicit recursive structures and low encoding and decoding complexity. Using some powerful decoders, polar codes can outperform the LDPC and turbo codes in error correcting performance. These advantages have enabled polar codes to sever as the coding scheme for control channels in 5G communication scenarios. By the polarization operation on N independent uses of a B-DMC W, N synthesized bit-channels with various reliabilities are produced. It may be convenient to realize a simple UEP through assigning more important information bits to the most reliable bit-channels. This mapping relationship between bit-channel reliability and importance level is utilized in [4]. It is an obvious advantage of polar codes compared to other coding schemes. Considering the error propagation problem in the successive cancellation decoding, a modified construction method of polar codes is proposed in [5] to improve UEP performance. However, it gives no explicit designs for other powerful decoding algorithms.

In many communication systems, the channel state information is not always available at the link terminals. For efficient transmission over the time-varying channels, rateless coding is a flexible technique to adapt to the situation where the real-time parameters of channels are unknown at the transmitter. The coded channel symbols are transmitted in a way of incremental redundancy until all the message can be recovered successfully. LT codes [6] and raptor codes [7]

The associate editor coordinating the review of this manuscript and approving it for publication was Wen Chen.

are both classical rateless codes. In particular, spinal codes are a new class of rateless codes, proposed by Perry et al. in [8]. The information bits are first divided into multiple segments and then each one is put into a hash function continuously to generate pseudo-random bits, which are mapped to channel symbols and then transmitted pass by pass. It has been proven that spinal codes are capable of capacity-approaching over binary symmetric channel (BSC) and additive white Gaussian noise (AWGN) channel, especially at low signal-to-noise ratio (SNR). Moreover, spinal codes can modify the code rate adaptively in the time-varying channels to achieve higher bandwidth efficiency. These merits make spinal codes qualified to be an advanced channel coding scheme for 5G-NR communications.

Additionally spinal codes have potential UEP property due to their serial coding structure. Based on the feature, literature [9] proposed a UEP scheme where the different importance levels are encoded in order and assigned different rates. However, the last part will always receive the worst protection. The UEP for all priority levels needs be enhanced.

Motivated by above observation, we explore a novel rateless coding scheme with improved UEP property by concatenating systematic polar codes (SPC) and spinal codes. Focusing on this work, our paper mainly provides following contributions:

- First, a novel concatenated polar-spinal coding scheme is designed to achieve a goal of better UEP for the information having different reliability requirements. To be specific, SPC are used as the outer codes and spinal codes are the inner codes in the encoding process.
- At the receiver, since the error-prone part in spinal coding always locates in the last few bits, a tail cyclic redundancy check (CRC)-aided Bubble decoding (CA-BD) is proposed to improve the performance of spinal codes effectively. It contributes to an enhanced UEP for all importance levels without the degraded performance of the lowest importance level.
- Moreover, the designed rateless transmission control in the proposed coding scheme is suitable for transmissions in the time-varying channels. Compared to the UEP spinal scheme, the total complexity of joint concatenation decoding process is reduced.
- Consequently numerical simulation demonstrates the proposed UEP polar-spinal coding and decoding schemes are able to achieve better UEP performance than some existing UEP rateless coding schemes, such as UEP-LT and UEP-raptor codes.

The remainder of this paper is organized as follows. Some preliminaries of polar codes and spinal codes are introduced in Section II, where their UEP properties are also demonstrated. Then, in Section III, we present the proposed rateless polar-spinal coding scheme and CA-BD algorithm in detail, and the rateless transmission process is designed as well. Section IV analyzes the UEP performance of the proposed schemes and gives the simulation results. Finally, Section V concludes the work in this paper.

II. POLAR CODES AND SPINAL CODES AND THEIR UEP EXPLORATION

This section introduces necessary backgrounds about construction and main decoding algorithms of polar codes and spinal codes. They lay the foundation for the design of the novel coding scheme and decoding algorithm. The UEP properties of polar and spinal are also explored in this section.

A. POLAR CODES

Encoding: Polar codes were proposed based on the channel polarization theory. Consider a BI-DMC $W : \mathcal{X} \to \mathcal{Y}$ with input alphabet $\mathcal{X} = \{0, 1\}$ and output alphabet $\mathcal{Y}$. For the polar code construction of length $N = 2^n, n = 1, 2, \ldots$ in the DMC W, N binary-input synthesized channels $W_N^{(i)}(i \in \mathbb{N} = \{1, 2, \ldots, N\})$ are derived through the recursive channel combining and splitting operations on N independent uses of DMC. We refer to $W_N^{(i)}$ as the i-th bit-channel. Assume that the vector $\boldsymbol{u}_N = (u_1, u_2, \ldots, u_N)$ is the source bit block, vectors $\boldsymbol{x}_N$ and $\boldsymbol{y}_N$ are referred to as the coded bits and received signals, respectively. $W_N^{(i)}(y_1^N, u_1^{i-1}|u_i)$ denotes the channel transition probability of the bit-channel $W_N^{(i)}$, which is calculated by

$$W_N^{(i)}(y_1^N, u_1^{i-1}|u_i) = \sum_{u_{i+1}^N} \frac{1}{2^{N-1}} W_N(y_1^N|u_1^N), \tag{1}$$

where $W_N(y_1^N|u_1^N) = \prod_{i=1}^{N} W(y_i|x_i)$, and $W(y|x)$ is the transition probability of W. The capacity of each bit-channel gets polarized. That is, bits transmitted on these bit-channels either experience almost noiseless channels or almost completely noisy channels as N gets large. Then, the polar coding is performed by choosing the most reliable K bit-channels to convey the information bits. The remaining bit-channels will be used to carry the fixed frozen bits which are known to the receiver. The coding rate is $R = K/N$. To determine the bit-channel set for information bits, effective sorting algorithms, such as Density Evolution algorithm [10], Gaussian approximation (GA) [11], can be utilized.

Suppose that $\mathcal{A}$ and $\mathcal{A}^{\mathcal{C}}$ denote the index set of information bits and frozen bits, respectively. Mathematically, the polar codeword $\boldsymbol{c}_N$ of $\mathcal{C}_{\text{polar}}(N, K, \mathcal{A})$ is formulated by

$$\boldsymbol{c}_N = \boldsymbol{u}_N \boldsymbol{G}_N = \boldsymbol{u}_N \boldsymbol{F}_2^{\otimes n}, \tag{2}$$

where $\boldsymbol{G}_N$ is the generator matrix of N-dimension, $\boldsymbol{F}_2^{\otimes n}$ denotes the n-th Kronecker power of $\boldsymbol{F}_2 = \begin{bmatrix} 1 & 0 \\ 1 & 1 \end{bmatrix}$.

The general polar code could be transformed into its corresponding systematic pattern. One class of systematic polar codes were constructed in [12] by specifying a set of indices of the codeword $\boldsymbol{c}_N$ as the indices transmitting the information bits. The message $\boldsymbol{u}_N$ waiting for encoding can be divided into two parts $\boldsymbol{u}_{\mathcal{A}}$ and $\boldsymbol{u}_{\mathcal{A}^{\mathcal{C}}}$; then, the codeword $\boldsymbol{c}_N$ is rewritten as

$$\boldsymbol{c}_N = \boldsymbol{u}_{\mathcal{A}} \boldsymbol{G}_{\mathcal{A}} + \boldsymbol{u}_{\mathcal{A}^{\mathcal{C}}} \boldsymbol{G}_{\mathcal{A}^{\mathcal{C}}}, \tag{3}$$

where $\boldsymbol{G}_{\mathcal{A}}$ denotes a submatrix consisting of some rows of $\boldsymbol{G}_N$, and the row indices are determined by $\mathcal{A}$. Assume that the indices of systematic and parity blocks of $\boldsymbol{c}_N$ are labeled by $\mathcal{B}$ and $\mathcal{B}^{\mathcal{C}} = \mathbb{N}\backslash\mathcal{B}$, respectively. The corresponding systematic bits $\boldsymbol{c}_{\mathcal{B}}$ and parity bits $\boldsymbol{c}_{\mathcal{B}^{\mathcal{C}}}$ can be derived by

$$\boldsymbol{c}_{\mathcal{B}} = \boldsymbol{u}_{\mathcal{A}}\boldsymbol{G}_{\mathcal{A}\mathcal{B}} + \boldsymbol{u}_{\mathcal{A}^{\mathcal{C}}}\boldsymbol{G}_{\mathcal{A}^{\mathcal{C}}\mathcal{B}}, \tag{4}$$

$$\boldsymbol{c}_{\mathcal{B}^{\mathcal{C}}} = \boldsymbol{u}_{\mathcal{A}}\boldsymbol{G}_{\mathcal{A}\mathcal{B}^{\mathcal{C}}} + \boldsymbol{u}_{\mathcal{A}^{\mathcal{C}}}\boldsymbol{G}_{\mathcal{A}^{\mathcal{C}}\mathcal{B}^{\mathcal{C}}}, \tag{5}$$

where $\boldsymbol{G}_{\mathcal{A}\mathcal{B}}$ is a submatrix of $\boldsymbol{G}_N$ with row indices belonging to $\mathcal{A}$ and column indices belonging to $\mathcal{B}$. Other submatrices are similarly denoted. When the frozen bits are fixed as all-zeros, we formulate (5) to that

$$\boldsymbol{c}_{\mathcal{B}^{\mathcal{C}}} = \boldsymbol{u}_{\mathcal{A}}\boldsymbol{G}_{\mathcal{A}\mathcal{B}^{\mathcal{C}}}, \tag{6}$$

and

$$\boldsymbol{u}_{\mathcal{A}} = (\boldsymbol{c}_{\mathcal{B}} - \boldsymbol{u}_{\mathcal{A}^{\mathcal{C}}}\boldsymbol{G}_{\mathcal{A}^{\mathcal{C}}\mathcal{B}})(\boldsymbol{G}_{\mathcal{A}\mathcal{B}})^{-1} = \boldsymbol{c}_{\mathcal{B}}(\boldsymbol{G}_{\mathcal{A}\mathcal{B}})^{-1}. \tag{7}$$

From (6) (7), it is seen that $\boldsymbol{c}_{\mathcal{B}^{\mathcal{C}}}$ exists only if $\mathbf{G}_{\mathcal{A}\mathcal{B}}$ is invertible. Here the configuration $\mathcal{B} = \mathcal{A}$ is used to ensure an invertible $\mathbf{G}_{\mathcal{A}\mathcal{B}}$ according to [12].

Decoding: Successive cancellation (SC) decoding algorithm of polar codes was proposed in [3]. The SC decoder estimates the source set successively from u_1 to u_N. The frozen bits are already known to the receiver, hence the SC decoder only needs to recover each information bit by the decision

$$\hat{u}_i = \begin{cases} 0, & L_N^{(i)}(\hat{u}_i) \geqslant 0 \\ 1, & L_N^{(i)}(\hat{u}_i) < 0, \end{cases} \tag{8}$$

where

$$L_N^{(i)}(\hat{u}_i) = \log \frac{W_N^{(i)}(y_1^N, \hat{u}_1^{i-1} | u_i = 0)}{W_N^{(i)}(y_1^N, \hat{u}_1^{i-1} | u_i = 1)} \tag{9}$$

is the log-likelihood ratio (LLR) corresponding to estimated value $\hat{u}_i (i \in \mathcal{A})$. The complexity of SC decoding is $O(N \log N)$.

One bit decision error will be propagated to the following bits over the multi-layer coding graph, SC does not perform well when the code length is finite. Fortunately some modified SC-based decoding algorithms such as SC-List (SCL) decoding [13] were proposed. In each level of list decoding, the SCL decoder doubles the number of decoding path and then reserves the most reliable *List* paths as candidate output. The total complexity increases to $O(List \cdot N \log N)$, which is *List* times that of SC decoding. In [14], a CRC-aided SCL decoding (CA-SCL) was proposed. SCL decoder checks each candidate path with the concatenated CRC and outputs the path passing CRC, so as to attain significant performance gain.

B. SPINAL CODES

Encoding: The encoding structure of spinal codes is shown in Fig. 1. First, the encoder divides the n-bit message block $\mathbf{m}$ into d $(d = n/k)$ sub-blocks $[\bar{\mathbf{m}}_1, \bar{\mathbf{m}}_2, \ldots, \bar{\mathbf{m}}_{n/k}]$, each of which consists of k bits. These sub-blocks are sequentially

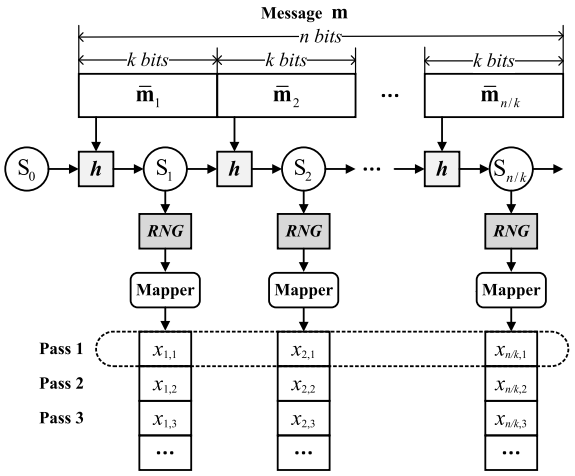

FIGURE 1. The structure of spinal coding.

input to a hash function $h(\cdot)$ in order, generating a series of v-bit hash states S_i,

$$S_i = h(S_{i-1}, \bar{\mathbf{m}}_i), \quad i = 1, 2, \ldots, n/k. \tag{10}$$

The initial state S_0 is the zero set of v-dimension, which is known by both the encoder and the decoder. Then, these states work as seeds for pseudo random number generators (RNG) to output a sequence of c-bit random numbers, i.e., $RNG : \{0,1\}^v \times L \rightarrow \{0,1\}^c$, where L is the number of passes. Ultimately the mapping functions convert these random bits into channel symbols $\boldsymbol{x}_i = \{x_{i,j}, 1 \leqslant j \leqslant L\}$. The symbols are transmitted pass by pass over the channel.

Decoding: Spinal codes can perform the maximum likelihood (ML) decoding based on a decoding tree to recover the message. The decoding tree has d depths. From the root node, 2^k branches are expanded corresponding to the 2^k child nodes at each node until it comes to the last depth. Specifically, we reuse the same initial hash state S_0, the hash function and RNG to reproduce all 2^n possible pathes of the decoding tree. The ML Spinal decoding is to search for the encoded message that has the least path metric to the received symbols, i.e., the minimum distance decoding principle. For the message $\mathbf{m}$ and its corresponding estimation $\hat{\mathbf{m}}$, the decoding result is presented as follows:

$$\hat{\mathbf{m}} = \underset{\mathbf{m}' \in (0,1)^n}{\arg\min} \left\| \bar{\boldsymbol{y}} - \bar{\boldsymbol{x}}(\mathbf{m}') \right\|, \tag{11}$$

where $\bar{\boldsymbol{y}}$ denotes the received signal vector and $\bar{\boldsymbol{x}}$ is the encoded symbol vector corresponding to the possible message vector $\mathbf{m}' \in (0,1)^n$.

However, the complexity of the optimal ML decoding increases exponentially. In order to decrease the decoding complexity, an improved Spinal decoder named as Bubble decoder is designed in [8], which is an approximate ML decoding through pruning the decoding tree. In this decoding process, only a maximum of B branches $\mathbb{B}_i (i \leqslant d)$ with the minimum cost are preserved at each depth. Then, the decoder expands $B \cdot 2^k$ child nodes at the next depth of the tree,

and then similarly saves the B candidate paths after sorting. It repeats the above steps until the last depth. In the end, the Bubble decoder chooses the one with the lowest cost in the saved B paths as the decoding output.

The complexity of Bubble decoding is evaluated as $O(n \cdot B \cdot 2^k \cdot (v + k + \log B))$. Obviously, it is decreased in contrast to the exponential complexity to n of ML decoding. Using the stack decoding and hierarchical operation, another decoding algorithm [15] reduced the decoding complexity maintaining the performance of spinal codes.

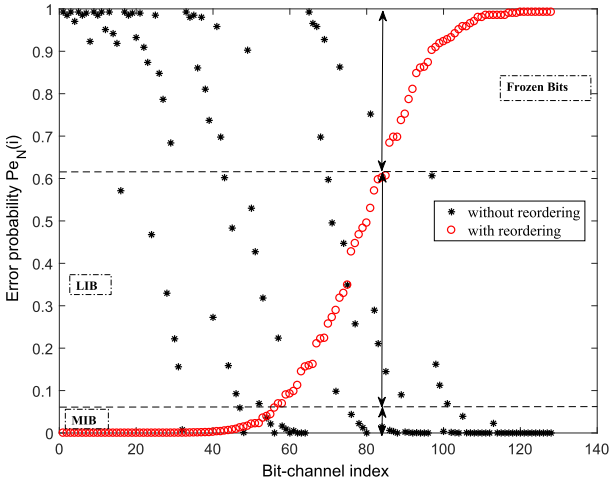

FIGURE 2. Error probability distribution of bit-channels in an AWGN channel, $N = 128$.

C. UNEQUAL ERROR PROTECTION PROPERTY

Through the channel combining and splitting operations, a series of bit-channels with various reliabilities are formulated for the polar code construction. Fig. 2 shows the error probability $Pe_N(i)$ distribution of each bit-channel and that of ordering, where $Pe_N(i)$ is calculated by GA algorithm in the AWGN channel.

Based on the property, it may be convenient to employ UEP for the different importance levels by mapping between reliability of bit-channel and importance of bit. Specifically, we assume that the message bits are divided into two importance levels. One part with the higher reliability requirement has superior importance level, termed the more important bits (MIB). Another part having the lower reliability requirement is called less important bits (LIB). The more reliable information bit-channels are assigned to carry the MIB; the remaining reliable ones convey the LIB (see Fig. 2). Fig. 3 presents the UEP performance of polar codes under SC and CA-SCL decoding. We can see that polar codes have good inherent UEP property by the mapping operation. Additionally this is achieved without any significant modification to the procedures of encoding and decoding. The similar UEP schemes were applied to the JPEG2000 compression technique based on turbo codes or polar codes [2], [4]. Their resulting performance demonstrated the advantages of UEP over the conventional EEP transmission.

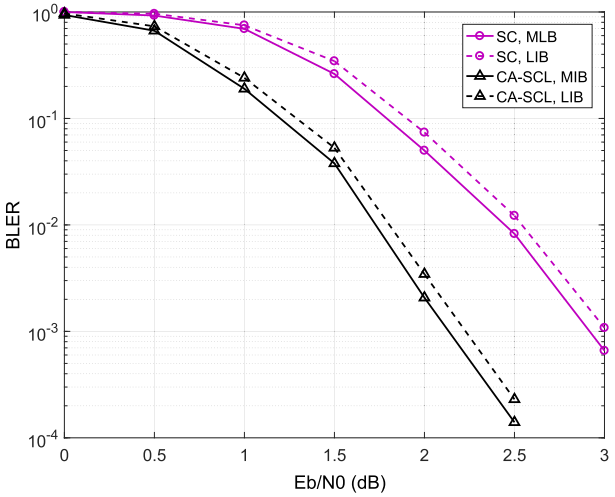

FIGURE 3. The UEP performance of polar codes under SC and CA-SCL decoders over the AWGN channel, where polar code length $N = 1024$, $R = 1/2$, the ratio of MIB is $r_M = 0.125$; 4-bit CRC and $L = 4$ are used for CA-SCL.

As for spinal code, it possesses potential UEP property as well. Since spinal code performs encoding the message sub-blocks successively, only the channel input sets $\boldsymbol{x}_i, \boldsymbol{x}_{i+1}, \ldots \boldsymbol{x}_d$ contain the information of $\bar{\mathbf{m}}_i$. For example, the information of the first sub-block $\bar{\mathbf{m}}_1$ is conveyed by all the symbols $\boldsymbol{x}_1, \boldsymbol{x}_2, \ldots \boldsymbol{x}_d$. However, the last one $\bar{\mathbf{m}}_d$ is only transmitted by the symbols $\boldsymbol{x}_d$. For given L passes, the number of symbols related to any later sub-block will decrease. It is concluded that the previous sub-block is able to be better protected compared to the following ones.

In this work, let K_M and K_L denote the numbers of MIB and LIB, respectively. The corresponding information bit-channel indices assigned to MIB and LIB are included in set $\mathcal{A}_M$ and $\mathcal{A}_L$, which are subsets of $\mathcal{A}_N$. r_M and r_L denote the ratios of MIB and LIB to all information bits, respectively, where $r_M = K_M/K_0$, $K_0 = K_M + K_L$, and $r_L = 1 - r_M$. In this paper, we will inherit the UEP property of polar codes and spinal codes for enhanced UEP performance.

III. PROPOSED UEP RATELESS POLAR-SPINAL CODING AND DECODING SCHEMES

In this section, we propose a novel concatenated UEP coding scheme based on SPC and rateless spinal codes. Meanwhile, a CRC-aided Bubble decoding algorithm is proposed to improve the performance of the coding scheme. Additionally, the rateless transmission procedure in the time-varying channels is designed. We first consider the case of two importance levels. The proposed scheme can be easily extended to a general case of more levels.

A. UEP POLAR-SPINAL CODING SCHEME

The proposed cascading coding scheme uses SPC as the outer codes, spinal codes as the inner codes. Each importance level information is first encoded by the CRC, and the check bits are attached to the importance level. Then, as shown in Fig. 4,

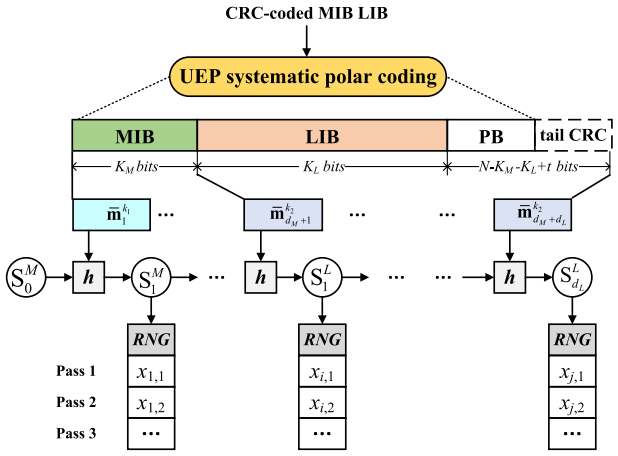

FIGURE 4. The proposed UEP polar-spinal coding scheme.

K_M-bit MIB and K_L-bit LIB including the CRC parity bits are encoded into the codeword $\boldsymbol{c}_N$ of $\mathcal{C}_{\text{SPC}}(N, K_0, \mathcal{A})$. Note that the UEP property of polar codes should be employed, i.e., the MIB are assigned on the K_M most reliable bit-channels. For SPC, assume that systematic bits $\boldsymbol{c}_{\mathcal{B}_M}$ are the MIB, and $\boldsymbol{c}_{\mathcal{B}_L}$ are the LIB. $\mathcal{B}_M$ and $\mathcal{B}_L$ are the index sets of MIB and LIB in the $\boldsymbol{c}_N$, respectively. The coding process is executed by that

$$\boldsymbol{c}_{\mathcal{B}_M} = \boldsymbol{u}_{\mathcal{A}_M}\mathbf{G}_{\mathcal{A}_M\mathcal{B}_M} + \boldsymbol{u}_{\mathcal{A}_L}\mathbf{G}_{\mathcal{A}_L\mathcal{B}_M} + \boldsymbol{u}_{\mathcal{A}^c}\mathbf{G}_{\mathcal{A}^c\mathcal{B}_M}, \quad (12)$$

$$\boldsymbol{c}_{\mathcal{B}_L} = \boldsymbol{u}_{\mathcal{A}_M}\mathbf{G}_{\mathcal{A}_M\mathcal{B}_L} + \boldsymbol{u}_{\mathcal{A}_L}\mathbf{G}_{\mathcal{A}_L\mathcal{B}_L} + \boldsymbol{u}_{\mathcal{A}^c}\mathbf{G}_{\mathcal{A}^c\mathcal{B}_L}, \quad (13)$$

$$\boldsymbol{c}_{\mathcal{B}^c} = \boldsymbol{u}_{\mathcal{A}_M}\mathbf{G}_{\mathcal{A}_M\mathcal{B}^c} + \boldsymbol{u}_{\mathcal{A}_L}\mathbf{G}_{\mathcal{A}_L\mathcal{B}^c} + \boldsymbol{u}_{\mathcal{A}^c}\mathbf{G}_{\mathcal{A}^c\mathcal{B}^c}. \quad (14)$$

According to (6) (7), we obtain that

$$\boldsymbol{u}_{\mathcal{A}_M\cup\mathcal{A}_L} = \boldsymbol{c}_{\mathcal{B}_M\cup\mathcal{B}_L}(\mathbf{G}_{(\mathcal{A}_M\cup\mathcal{A}_L)(\mathcal{B}_M\cup\mathcal{B}_L)})^{-1}, \quad (15)$$

$$\boldsymbol{c}_{\mathcal{B}^c} = \boldsymbol{u}_{\mathcal{A}_M\cup\mathcal{A}_L}\mathbf{G}_{(\mathcal{A}_M\cup\mathcal{A}_L)\mathcal{B}^c}. \quad (16)$$

Thus it is required that the matrix $\mathbf{G}_{(\mathcal{A}_M\cup\mathcal{A}_L)(\mathcal{B}_M\cup\mathcal{B}_L)}$ is invertible for the UEP systematic polar coding. We can ensure that by setting $\mathcal{A}_M = \mathcal{B}_M, \mathcal{A}_L = \mathcal{B}_L$.

Next, the polar codeword is put into the spinal encoder. Since the polar code of systematic pattern is utilized as the outer code, the polar coded bits continue to be divided into various importance levels before spinal coding. To further enhance the UEP, the more important part is first processed. To be more specific, the $\boldsymbol{c}_{\mathcal{B}_M}$ are divided into d_M sub-blocks $[\bar{\mathbf{m}}_1^{k_1}, \bar{\mathbf{m}}_2^{k_1}, \ldots \bar{\mathbf{m}}_{d_M}^{k_1}]$, each of which consists of k_1 bits. The LIB $\boldsymbol{c}_{\mathcal{B}_L}$ along with total parity bits (PB) are divided into d_L sub-blocks $[\bar{\mathbf{m}}_{d_M+1}^{k_2}, \bar{\mathbf{m}}_{d_M+2}^{k_2}, \ldots \bar{\mathbf{m}}_{d_M+d_L}^{k_2}]$, each one including k_2 bits. Every sub-block is input into the hash function h in order. We obtain the resulting hash values $[S_1^M, S_2^M, \ldots, S_{d_M}^M]$ and $[S_1^L, S_2^L, \ldots, S_{d_L}^L]$, $S_0^M = S_0$ and $S_0^L = S_{d_M}^M$. In the sequel, all the hash values pass through the RNG and are mapped into the channel input symbols $\boldsymbol{x}_1, \boldsymbol{x}_2, \ldots$.

Assuming that L passes are transmitted, the numbers of symbols used for decoding MIB and LIB are $L(d_M + d_L)$ and Ld_L, respectively. The corresponding spinal code rates (bit/channel use) of MIB and LIB are $R_M = k_1 d_M / L(d_M + d_L)$, $R_L = k_2 d_L / L d_L$. Note that it should satisfy that $R_M < R_L$ for UEP. Therefore we set the condition that $k_1 \leqslant k_2$ to further guarantee the UEP property of the above coding process.

B. TAIL CRC-AIDED BUBBLE DECODING ALGORITHM

In this subsection, we propose a new decoding algorithm to improve the performance of both MIB and LIB.

When receiving the channel output signals, the receiver first executes the inner spinal decoding. If the Bubble decoder is adopted, conventionally, the estimated message with the minimum path cost (see Equ. (11)) is used as the decoding output. However, to improve the decoding performance, we propose a CRC-aided Bubble decoding (CA-BD) algorithm where the concatenated CRC code is applied to select the most possible path. At the last depth of the decoding tree, the saved B candidate pathes are checked by CRC decoder after bubble sorting, then the decoder outputs the first path that can pass the CRC detection as the recovered results. If there is no path passing the check, the decoder still uses the message with the minimum path cost as the decoding output.

Furthermore, we consider the UEP property of spinal codes to optimize the CA-BD. According to [16], the block error rate (BLER) performance of inner spinal code $\mathcal{C}_{\text{spinal}}(n, k, L)$ for message $\mathbf{m}$ is calculated by

$$\begin{aligned}\text{BLER} &= 1 - \text{P}(\hat{\mathbf{m}} = \mathbf{m}) \\ &= 1 - \text{P}(\hat{\bar{\mathbf{m}}}_1 = \bar{\mathbf{m}}_1, \ldots, \hat{\bar{\mathbf{m}}}_d = \bar{\mathbf{m}}_d) \\ &= 1 - \prod_{i=1}^{d}(1 - \Omega_i), \end{aligned} \quad (17)$$

where $\hat{\bar{\mathbf{m}}}_i$ denotes the estimation of $\bar{\mathbf{m}}_i$, and

$$\Omega_i = \text{P}(\hat{\bar{\mathbf{m}}}_i \neq \bar{\mathbf{m}}_i | \hat{\bar{\mathbf{m}}}_1 = \bar{\mathbf{m}}_1, \ldots, \hat{\bar{\mathbf{m}}}_{i-1} = \bar{\mathbf{m}}_{i-1}).$$

Particularly the error probability of last sub-block Ω_d is a lower bound of BLER, i.e., $\text{BLER} \geqslant \Omega_d$. In fact, Ω_d could be regarded as the error probability of a short spinal code $\mathcal{C}_{\text{spinal}}(k, k, L)$. Since the message $\bar{\mathbf{m}}_d$ is only carried by the symbols $\boldsymbol{x}_d$ and independent of $\boldsymbol{x}_i$ $(1 \leqslant i \leqslant d-1)$, the information in $\bar{\mathbf{m}}_d$ obtains the least protection from the spinal codes, easily suffering errors in the transmissions.

The total protection for the whole systematic polar codeword may consume large CRC redundant bits in the CA-BD. Based on above considerations, we only perform CRC coding to the last sub-block and add t parity bits at the tail of the message block, as shown in Fig. 4. In consequence, the error-prone last sub-block acquires enhanced protection. The performance of both MIB and LIB will be improved effectively.

With regard to the decoding of outer codes SPC, we adopt the powerful CA-SCL decoding (CA-SD). The CRC coded bits included in each importance level can be utilized to select survival path of *List* candidate paths in the SCL decoding. The path that passes the checks of all importance levels is chosen as the output results.

The joint concatenated decoding algorithm at the receiver is described in Algorithm 1. In the algorithm, the symbol

flag denotes an indicator, $flag \in [0, 1]$; $tail - \mathcal{CRC}(\cdot)$ and $\mathcal{CRC}(\cdot)$ are the functions generating a binary output to indicate whether the path passes the CRC detection or not. Specifically the output "1" reveals that the path is checked successfully. $I_i^{(\cdot)}$ denotes the information bits of each importance level on the i-th path.

Algorithm 1 Joint CA-BD and CA-SD

Input: the reserved B paths $\mathbb{B}_d$ of Bubble decoding at the last depth d;
for $i = 1 : B$ **do**
  Perform tail-CRC for the i-th path p_i in $\mathbb{B}_d$;
  Tail-CRC check result: $flag_1^i \leftarrow tail - \mathcal{CRC}(p_i)$;
  CRC check for the systematic message of each importance level: $flag_2^i \leftarrow \mathcal{CRC}(I_i^{(M)}) \cap \mathcal{CRC}(I_i^{(L)})$;
  if $flag_1^i == 1 \&\& flag_2^i == 1$ **then**
    output $\hat{p} = p_i$, and the receiver sends an ACK (acknowledge) signal;
    break;
if *all* $flag_2^i == 0$ *for* $i \in [1, 2, .., B]$ **then**
  output one path p_l that passes tail CRC or with the lowest path cost;
Perform SCL decoding to the spinal decoded p_l; Save *List* paths $\mathbb{S}$ in SCL decoding;
for $j = 1 : List$ **do**
  check the path q_j: $flag_3^j \leftarrow \mathcal{CRC}(I_j^{(M)}) \cap \mathcal{CRC}(I_j^{(L)})$;
  if $flag_3^j == 1$ **then**
    output $\hat{q} = q_j$, and the receiver sends an ACK;
    break;
if *all* $flag_3^j == 0, j \in [1, 2, \ldots, List]$ **then**
  output the path $\hat{q} = q_l$ with the lowest path cost.

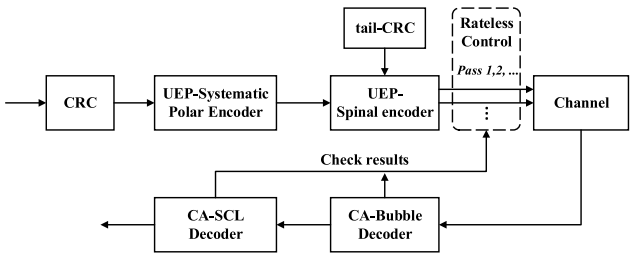

FIGURE 5. The proposed polar-spinal coding and decoding structure.

C. DESIGN OF RATELESS TRANSMISSION PROCESS

Our proposed polar-spinal coding and decoding procedure is shown in Fig. 5. It is described as follows:

- The MIB and LIB are first separately encoded by the CRC encoder and the CRC check bits are attached to the tail of MIB block and LIB block (including K_M bits and K_L bits, respectively). Then, all the information blocks are together encoded into a UEP systematic polar code $\mathcal{C}_{\text{SPC}}(N, K_M + K_L, \mathcal{A})$.
- The SPC codeword is first divided into multiple sub-blocks in order according to the bit importance levels, i.e., $[\bar{\mathbf{m}}_1^{k_1}, \bar{\mathbf{m}}_2^{k_1}, \ldots \bar{\mathbf{m}}_{d_M}^{k_1}]$ and $[\bar{\mathbf{m}}_{d_M+1}^{k_2}, \bar{\mathbf{m}}_{d_M+2}^{k_2}, \ldots \bar{\mathbf{m}}_{d_M+d_L}^{k_2}]$. The last sub-block of the LIB is encoded by t-bit CRC (here, $t = k_2$ is set), and the check bits are attached to the tail sub-block. Then, all the sub-blocks are put into the inner spinal encoder with $\mathcal{C}_{\text{spinal}}(N + t, [k_1, k_2], L)$. The output symbols $\boldsymbol{x}_1, \boldsymbol{x}_2, \ldots \boldsymbol{x}_{d_M+d_L}$ are transmitted pass by pass over an unknown channel.
- At the receiver, the received signals are first decoded by the CA-Bubble decoder. If the decoding fails, the CA-BD results are put into the CA-SCL decoder to recover the message. The whole decoding process follows the Algorithm 1. If the message cannot be recovered successfully with the transmitted passes, the transmitter will incrementally send symbols by pass until an ACK feedback is received.

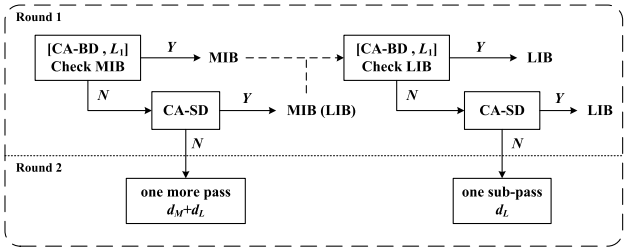

FIGURE 6. The rateless transmission and control process in the UEP polar-spinal coding scheme.

It is notable that the proposed polar-spinal coding scheme still consists of a rateless coding process. The rateless transmission and control are described in detail in the Fig. 6, which also take into account the goal of UEP. The order of information checking and rateless transmissions involve that of the priority levels.

- Assume that in the Round 1, L_1 passes have been transmitted to the receiver and CA-BD is performed. The decoded MIB are first checked by the CRC. If MIB can pass the check, they are output as the recovered message, and we continue to check the LIB. Otherwise, CA-SD would be activated to correct the errors in MIB. Note that the LIB may be also recovered successfully in this CA-SD. However, if this outer decoding still fails, one more pass including $(d_M + d_L)$ symbols will be transmitted to the terminal in the Round 2. Then, the above procedure will continue.
- If the MIB are received successfully, the decoded LIB in the CA-BD of Round 1 are checked by CRC. If any errors are detected, the CA-SD is then executed, where the MIB recovered previously work as the known frozen bits. Assuming that the LIB cannot be decoded correctly, more symbols are required. However, the recovery of LIB is only related to the coded symbols corresponding to LIB due to the serial coding structure of spinal code. There is no need to transmit the coded previously

symbols corresponding to MIB. Therefore, only d_L symbols corresponding to LIB are sent in a sub-pass to the terminal in the Round 2. The above procedure will proceed until the LIB are recovered successfully.

Note that the concatenated CRC codes play an essential role in the proposed coding scheme. The main contributions are that i) in the practical applications, the CRC check bits concatenated to each importance level are employed to verify whether the information is recovered or not; ii) they are utilized to choose the survival path when the CA-SD of outer SPC is required; iii) the tail-CRC ensures that both MIB and LIB can obtain a performance improvement. Although some redundancy is introduced by CRC coding, the rate loss may be ignored as the message length gets large enough.

IV. ANALYSIS AND SIMULATION

In this section, we will analyze the performance of the proposed CA-BD and the UEP performance of rateless polar-spinal coding scheme. The complexity analysis is also discussed.

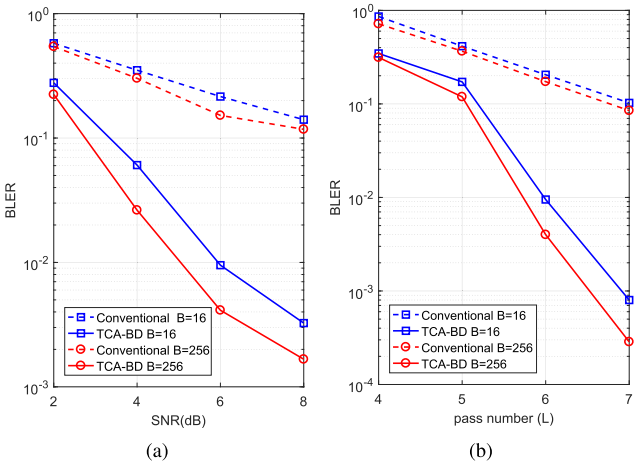

FIGURE 7. The BLER performance of proposed TCA-BD and conventional Bubble decoding vs. different SNR (a) and pass number (b), where $n = 24$, $k_1 = k_2 = 4$ and $B = 16, 256$ for spinal codes.

A. PERFORMANCE OF CA-BD

The BLER performance of proposed tail CA-BD (TCA-BD) is presented in Fig. 7, compared to the conventional Bubble decoding. In particular, Fig.7 (a) shows the results of BLER under different SNR with a fixed pass number $L = 6$; for a given SNR $= 3$ dB, the BLER performance vs. pass number is presented in Fig.7 (b). The message length is 24 bits, and $k_1 = k_2 = 4$ is set for the spinal codes. At the decoder, $B = 16$ and $B = 256$ are separately utilized. According to the simulated results, it is seen that the BLER of TCA-BD is significantly decreased compared to the conventional decoding. The gain gap gets obvious as the channel condition SNR or the pass number increases. In other words, for a given BLER, less passes are needed when the TCA-BD is employed, which contributes to a reduced decoding overhead and transmission delay. On the other hand, we find that using the TCA-BD with a bigger B could obtain more gain over the conventional decoder. It is concluded that only a few t-bit check bits are attached, but the performance of spinal decoding is improved significantly. When the TCA-BD is applied to the UEP polar-spinal scheme, the performance of each importance level will be enhanced.

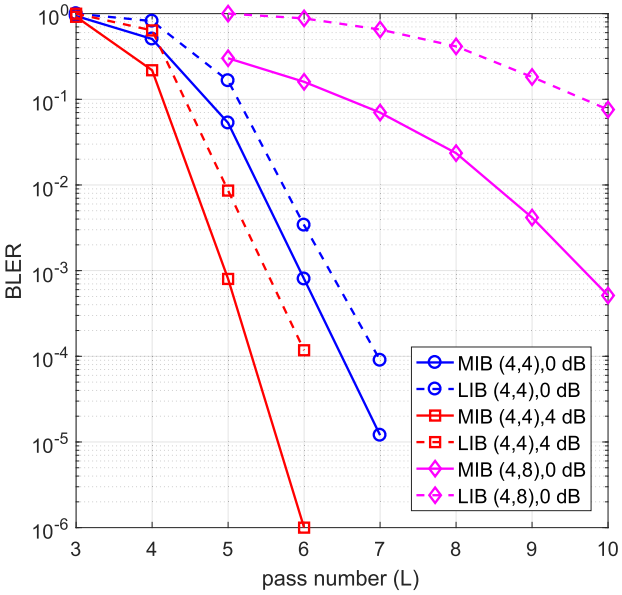

FIGURE 8. The BLER performance of MIB and LIB in the proposed UEP polar-spinal scheme, where SNR = 0 dB, 4 dB; $(k_1, k_2) = (4, 4), (4, 8)$.

B. UEP PERFORMANCE

We simulate the proposed UEP polar-spinal coding scheme in the AWGN channel under various SNR. The BLER results of MIB and LIB against pass number are showed in Fig. 8, where $K_M = 16, K_L = 28$ and each includes 6 CRC-bits. Polar code is with length $N = 64$, $List = 32$. $(k_1, k_2) = (4, 4), (4, 8)$, BPSK modulation and CA-BD with $B = 16$ are configured for spinal code. We can see that the UEP polar-spinal scheme possesses a good UEP performance when $k_1 = k_2$. Assuming the case of $k_1 < k_2$, the performance gap between MIB and LIB gets larger. That is, the MIB obtain more protection than the LIB, so as to have higher reliability in the communication. Compared to the UEP results of stand-alone polar codes in Fig. 3, the proposed polar-spinal scheme shows an enhanced UEP property.

Moreover, the UEP performances of some other existing UEP rateless coding schemes over the AWGN channel are provided in Fig. 9 for comparison. LT codes and raptor codes are other classical families of rateless codes. Specially raptor codes are also a class of concatenated rateless codes using outer high-rate LDPC codes and inner LT codes. Their UEP applications are explored in the literatures [17], [18] and the [19], respectively. The UEP LT coding scheme in [17] utilized an expanding window technique, and we call it LT-I. Reference [18] designed a UEP scheme for the noisy channel using LT codes, called LT-II.

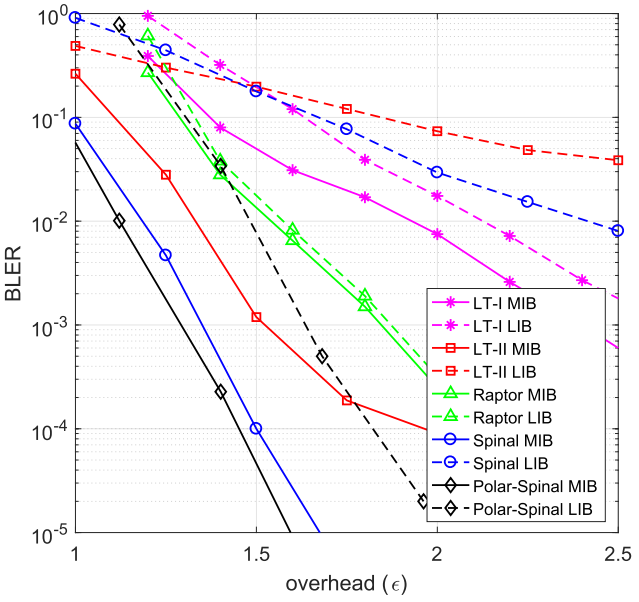

FIGURE 9. The UEP performances of the proposed polar-spinal scheme and the existing UEP schemes of rateless LT, raptor and spinal codes vs. the overhead.

For a fair comparison, the message length is $K_0 = 500$ bits, $r_M = 0.3$, and channel condition is SNR $= 8$ dB. For the polar-spinal code, $k_1 = k_2 = k = 4$, $N = 512$, CA-BD with $B = 16$ and CA-SD with $List = 32$ are set; for UEP spinal codes in [9], $k_1 = k_2 = k = 4$, $B = 16$; Belief Propagation decoding is used for LT and raptor codes. We show the BLER of MIB and LIB in each scheme versus the overhead. In terms of different rateless codes, the overhead is uniformly calculated by the ratio of the number of received transmitted symbols to the number of the message bits according to [17]. Specifically, the overhead is formulated by $\varepsilon_R = \varepsilon_L/R_L$ for the raptor codes, where ε_L is the overhead of inner LT codes and R_L is the coding rate of outer LDPC codes; $\varepsilon_S = L/k$ is for spinal codes; with regard to the UEP polar-spinal codes, the overhead is calculated by $\varepsilon_{P-S} = L(N+k)/k/K_0$.

We can see that our proposed UEP polar-spinal scheme outperforms other UEP schemes. The BLERs of both MIB and LIB are reduced. It is more evident particularly for the LIB part since the tail CA-BD is adopted. However, the UEP performances of the LT-I scheme and the raptor scheme are not obvious in the AWGN channel. Although the UEP LT-II scheme and UEP spinal codes could achieve a good UEP property, they improve the MIB performance at the cost of an impaired LIB performance.

C. COMPLEXITY ANALYSIS

In this subsection, we analyze the decoding complexity of proposed polar-spinal scheme and compare it with the existing UEP spinal, LT and raptor schemes. The Bubble decoding complexity is numerically dominant in the complexity of UEP scheme [9] using stand-alone spinal codes. It has the polynomial complexity of $C_B = O(\sum_{s=1}^{S} N_s \cdot B_s \cdot 2^{k_s} \cdot (v + k_s + \log B_s))$, where N_s is the bit number of s-th important level, and k_s and B_s denote the corresponding sub-block length and maximal number of reserved candidate branches, respectively. In the proposed polar-spinal scheme, the outer SPC may correct all of the errors in the decoding results of inner spinal codes, which avoids the requirement for one more round to transmit more passes or channel input symbols. Hence, the decoding times of spinal codes would be decreased and the rateless transmission delay and decoding delay are also reduced. Table. 1 presents some statistical ratios η of blocks unrecovered in CA-BD but corrected by the outer SPC in the decoding process of one transmission round. It is seen that the outer SPC works better in recovering the information as the SNR grows.

TABLE 1. Some results of the ratio η of blocks corrected by the outer SPC. The simulation parameters are same as the Fig. 9; the pass number is $L = 5$.

SNR(dB)	1	2	4	6
η	0.0928	0.1159	0.1337	0.1361

Assume that the complexity of CRC check can be negligible in the proposed scheme. The decoding complexity of SCL decoding is $C_P = O(List \cdot N\log N)$. In consideration of the given parameters used in Fig. 9, it is obvious that $C_P < C_S$. The proposed scheme may achieve a reduced complexity of about $\eta(C_S - C_P)$, compared to the UEP spinal scheme. Specifically, the polar-spinal scheme can provide about 12% reduction in complexity when SNR $= 6$ dB, while the UEP performance of polar-spinal is better than other rateless codes.

The LT and raptor with specific degree distribution (such as Ideal Soliton Distribution) have linear complexity using BP decoding in the simple erasure channel. For other practical construction, the complexity of LT using Robust Soliton Distribution is $C_{\mathrm{LT}} = O(K_0 \log K_0)$. When the LT and raptor are applied to the AWGN channel, their complexity would be increased. Although the UEP LT and raptor have lower complexity than the schemes using spinal codes, their UEP performances are unsatisfactory and are inferior to the proposed polar-spinal scheme consequently. In order to further decrease the complexity of proposed scheme, some improved decoding algorithms [15], [20] with significantly reduced complexity (the reduction is more than 40% in contrast to the Bubble decoding) can be utilized. In addition, the literature [8] optimized coding and decoding parameters of spinal codes: $k = 4$, $\log B = 8$, and a shorter message length. With the lower-complexity decoders and those optimal parameters, the complexity of the polar-spinal scheme may be acceptable in practice over the AWGN channel.

V. CONCLUSION

In this paper, a novel rateless coding scheme by utilizing outer SPC and inner spinal codes is proposed, which is demonstrated to have improved UEP property. In addition,

to eliminate the effect of error-prone part of spinal codes, a tail CA-BD algorithm is proposed to improve the performance of all importance levels. The ratelss transmission scheme is designed properly, and the complexity of joint concatenated decoding process is reduced compared to the stand-alone spinal coded UEP scheme. According to the simulated results in the AWGN channel, the proposed rateless polar-spinal coding approach is able to attain better UEP performance for each priority level than the existing UEP rateless coding schemes. The upcoming extensions of this work will include that the number of transmitted passes or coded symbols is adaptive for higher rate efficiency, and the specific design and analysis are explored for the fading channels.

REFERENCES

[1] V. Kumar and O. Milenkovic, "On unequal error protection LDPC codes based on Plotkin-type constructions," *IEEE Trans. Commun*, vol. 54, no. 6, pp. 994–1005, Jun. 2006.
[2] W. Zhang, X. Shao, M. Torki, A. HajShirMohammadi, and I. V. Bajic, "Unequal error protection of JPEG2000 images using short block length turbo codes," *IEEE Commun. Lett.*, vol. 15, no. 6, pp. 659–661, Jun. 2011.
[3] E. Arıkan, "Channel polarization: A method for constructing capacity-achieving codes for symmetric binary-input memoryless channels," *IEEE Trans. Inf. Theory*, vol. 55, no. 7, pp. 3051–3073, Jul. 2009.
[4] A. Hadi, E. Alsusa, and A. Al-Dweik, "Information unequal error protection using polar codes," *IET Commun.*, vol. 12, no. 8, pp. 956–961, May 2018.
[5] C. Cui, W. Xiang, Z. Wang, and Q. Guo, "Polar codes with the unequal error protection property," *Comput. Commun.*, vol. 123, pp. 116–125, Jun. 2018.
[6] M. Luby, "LT codes," in *Proc. 43rd IEEE Symp. Found. Comput. Sci. (FOCS)*, Nov. 2002, pp. 271–280.
[7] A. Shokrollahi, "Raptor codes," *IEEE Trans. Inf. Theory*, vol. 52, no. 6, pp. 2551–2567, Jun. 2006.
[8] J. Perry, P. A. Iannucci, K. E. Fleming, H. Balakrishnan, and D. Shah, "Spinal codes," in *Proc. ACM SIGCOMM*, Aug. 2012, pp. 49–60.
[9] X. Yu, Y. Li, W. Yang, and Y. Sun, "Design and analysis of unequal error protection rateless spinal codes," *IEEE Trans. Commun.*, vol. 64, no. 11, pp. 4461–4473, Nov. 2016.
[10] R. Mori and T. Tanaka, "Performance of polar codes with the construction using density evolution," *IEEE Commun. Lett.*, vol. 13, no. 7, pp. 519–521, Jul. 2009.
[11] P. Trifonov, "Efficient design and decoding of polar codes," *IEEE Trans. Commun.*, vol. 60, no. 11, pp. 3221–3227, Nov. 2012.
[12] E. Arıkan, "Systematic polar coding," *IEEE Commun. Lett.*, vol. 15, no. 8, pp. 860–862, Aug. 2011.
[13] I. Tal and A. Vardy, "List decoding of polar codes," *IEEE Trans. Inf. Theory*, vol. 61, no. 5, pp. 2213–2226, May 2015.
[14] K. Niu and K. Chen, "CRC-aided decoding of polar codes," *IEEE Commun. Lett.*, vol. 16, no. 10, pp. 1668–1671, Oct. 2012.
[15] W. Yang, Y. Li, X. Yu, and J. Li, "A low complexity sequential decoding algorithm for rateless spinal codes," *IEEE Commun. Lett.*, vol. 19, no. 7, pp. 1105–1108, Jul. 2015.
[16] W. Yang, Y. Li, X. Yu, and Y. Sun, "Two-way spinal codes," in *Proc. IEEE Int. Symp. Inf. Theory (ISIT)*, Barcelona, Spain, Jul. 2016, pp. 1919–1923.
[17] D. Sejdinović, D. Vukobratović, A. Doufexi, V. Šenk, and R. Piechocki, "Expanding window fountain codes for unequal error protection," *IEEE Trans. Commun.*, vol. 57, no. 9, pp. 2510–2516, Nov. 2009.
[18] I. Hussain, M. Xiao, and L. K. Rasmussen, "Unequal error protection of LT codes over noisy channels," in *Proc. Commun. Technol. Workshop (SweCTW)*, Oct. 2012, pp. 19–24.
[19] L. Yuan and J. An, "Design of UEP-raptor codes over BEC," *Eur. Trans. Telecommun.*, vol. 21, no. 1, pp. 30–34, 2010.
[20] Y. Hu, R. Liu, H. Bian, and D. Lyu, "Design and analysis of a low-complexity decoding algorithm for spinal codes," *IEEE Trans. Veh. Technol.*, vol. 68, no. 5, pp. 4667–4679, May 2019.

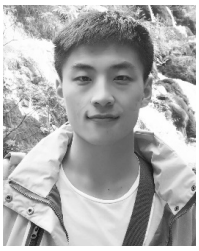

HAO LIANG received the B.S. degree in communication engineering from the College of Communications Engineering, PLA University of Science and Technology, Nanjing, China, in 2015, and the M.S. degree in communications and information system from the College of Communications Engineering, Army Engineering University of PLA (AEUPLA), Nanjing, in 2017, where he is currently pursuing the Ph.D. degree in information and communications engineering. His research interests include satellite communication, physical layer security, and channel coding, especially polar codes.

AIJUN LIU received the B.S. degree in microwave communications and the M.S. and Ph.D. degrees in communications engineering and information systems from the College of Communications Engineering, Nanjing, China, in 1990, 1994, and 1997, respectively. He is currently a Full Professor with the College of Communications Engineering, Army Engineering University of PLA. Since March 2015, he has been a Visiting Scholar with the Department of Electrical and Computer Engineering, University of Waterloo, Waterloo, ON, Canada. His current research interests include satellite communication system theory, signal processing, space heterogeneous networks, channel coding, and information theory.

FENGYI CHENG was born in Nanjing, Jiangsu, China, in 1988. He received the B.S. degree from Nanjing Post and Telecommunication University (NUPT), in 2011, and the M.S. degree in communication engineering and information systems from the College of Communications Engineering, Army Engineering University of PLA, Nanjing, in 2017, where he is currently pursuing the Ph.D. degree with the Institution of Communications Engineering. His research interests include satellite communication, coded modulation techniques, channel coding, and information theory.

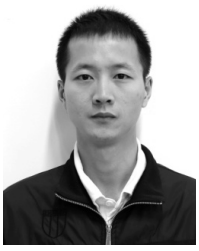

XIAOHU LIANG received the B.S. degree in communication engineering from the University of Electronic Science and Technology of China (UESTC), Chengdu, China, in 2011, and the Ph.D. degree in information and communications engineering from the PLA University of Science and Technology (PLAUST), Nanjing, China, in 2016. He visited Lund University for exchanging and researched the technique of Faster-than-Nyquist (FTN) signaling, in 2016. He is currently a Lecturer with Army Engineering University (AEU) and holds a postdoctoral position with the Department of Information Science and Engineering, Southeast University (SEU), Nanjing. His research interests include synchronization techniques for FTN signaling, spectrally efficient FDM (SEFDM), orthogonal time–frequency space (OTFS) modulation, and massive MIMO.